

Light Hadron Spectroscopy at BESIII*

Shuangshi Fang¹ (for the BESIII Collaboration)

¹ Institute of High Energy Physics, CAS, 100049, Beijing, China

Abstract: Based on the samples of 1.3×10^9 J/ψ events and 1.06×10^8 $\psi(3686)$ events taken at the BESIII detector, the recent progresses on the light meson spectroscopy, baryon spectroscopy and light meson decays are presented.

Key words: the BESIII detector, light hadron spectroscopy, charmonium decays

PACS: 13.20.Gd, 13.25.Gv, 14.40.Be

1 Introduction

At present our theoretical understanding of the light hadron spectrum remains based largely on the quark model due to the failure of the application of the perturbative theory in the low energy regime. In addition to the conventional hadrons predicted by the quark model, however, one of the clearest predictions of Quantum chromodynamics (QCD) is the presence of exotic hadrons, e.g., glueballs, multiquark states and hybrids. The search for these exotic states has been taken for many years and many candidates have been reported by different experiments, but none of them were unambiguously identified to date.

The J/ψ and $\psi(3686)$ decays have provided a wealth of information on the light hadron spectroscopy since they were discovered in 1970s. Due to their masses are below the charm meson pair, the direct decay into charmed mesons is forbidden, which offers a clean laboratory to study light hadron spectroscopy. Furthermore the comparison of the radiative and the hadronic decays provides not only insight into the decay mechanisms, but also helps in differentiating between the conventional $q\bar{q}$ states and the new spectroscopy.

In this talk, we present the progresses on the light meson spectroscopy, baryon spectroscopy and light meson decays based on the samples of 1.3×10^9 J/ψ events and 1.06×10^8 $\psi(3686)$ events collected with the BESIII detector.

2 Light meson spectroscopy

In 2005 the $X(1835)$ resonance was observed in $J/\psi \rightarrow \gamma\pi^+\pi^-\eta'$ [1], which then stimulated theoretical speculations on its nature. At BESIII, this structure was confirmed in the same decay channel [2] and other similar structures around 1.85 GeV/ c^2 were observed. To understand their nature, further study is strongly needed, in

particular, in searching for new decay modes.

In this talk, we present a study of $J/\psi \rightarrow \gamma K_S K_S \eta$ [3] decays using a sample of $(1310.6 \pm 10.5) \times 10^6$ J/ψ events collected with the BESIII detector. By requiring that $M_{K_S K_S}$ is in the $f_0(980)$ mass region, $M_{K_S K_S} \in [1.1, 1.15]$ GeV/ c^2 , the structure around 1.85 GeV/ c^2 shown in Fig. 1 (a) is clearly seen. A partial wave analysis (PWA) is performed and the spin parity of the $X(1835)$ is determined to be $J^{PC} = 0^{-+}$. The mass and width are measured to be $1844 \pm 9(\text{stat})_{-25}^{+16}(\text{syst})$ MeV/ c^2 and $192_{-17}^{+20}(\text{stat})_{-43}^{+62}(\text{syst})$ MeV, respectively, which are consistent with the results obtained by BESIII in $J/\psi \rightarrow \gamma\pi^+\pi^-\eta'$ [2].

Figure 1 (b) shows the comparison to the BESIII results of the masses and widths of the $X(p\bar{p})$, $X(1835)$, $X(1870)$, $X(1840)$ and $X(1810)$. The mass of $X(1840)$ is in agreement with $X(p\bar{p})$, while its width is significantly broader. Therefore, based on these data, one cannot determine whether $X(1840)$ is a new state or the signal of a $3(\pi^+\pi^-)$ decay mode of $X(p\bar{p})$. Further study, including an amplitude analysis to determine the spin and parity of the $X(1840)$, is needed to establish the relationship between these experimental observations.

In addition, we also performed the model-independent PWA of $J/\psi \rightarrow \gamma\pi^0\pi^0$. The results displayed in Fig. 2(b) indicate that the scalar contributions are mainly from $\sigma(600)$, $f_0(1370)$, $f_0(1500)$, $f_0(1710)$ and $f_0(2020)$. The production rate of the pure gauge scalar glueball in J/ψ radiative decays predicted by the lattice QCD [10] was found to be compatible with the production rate of J/ψ radiative decays to $f_0(1710)$; this suggests that $f_0(1710)$ has a larger overlap with the glueball compared to other glueball candidates (e.g., $f_0(1500)$). The tensor components, which is dominantly from $f_2(1270)$, also have a large contribution in $J/\psi \rightarrow \gamma\pi^0\pi^0$ decays.

Received 14 Sep. 2014

* This work is supported by National Natural Science Foundation of China (NSFC) under Contracts No. 11175189

1) E-mail: fangss@ihep.ac.cn

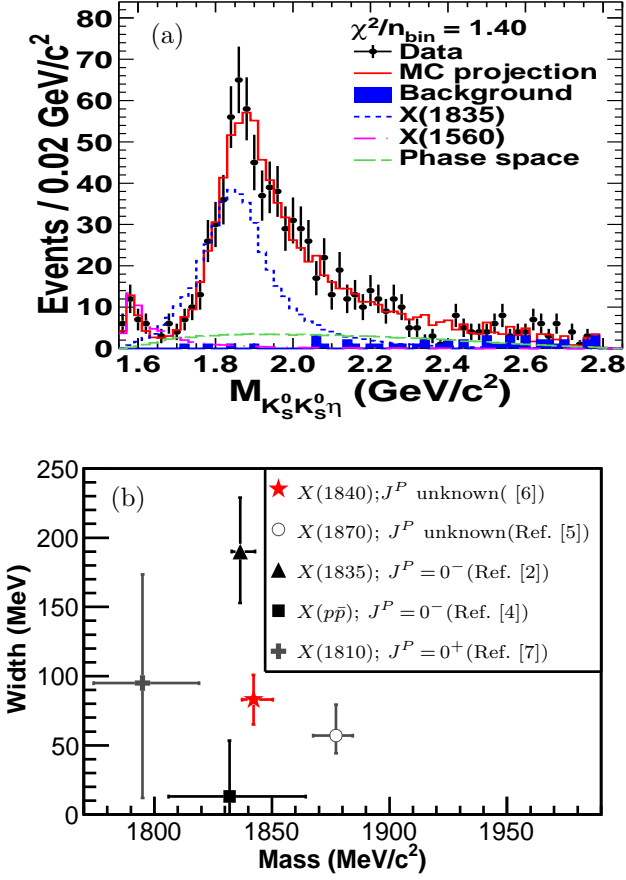


Fig. 1. (a) $K_S^0 K_S^0 \eta$ invariant mass spectrum for events with the requirement $M_{K_S^0 K_S^0} < 1.1 \text{ GeV}/c^2$ and PWA projections; (b) comparisons of observations at BESIII. The error bars include statistical, systematic, and, where applicable, model uncertainties.

3 Baryon spectroscopy

To search for new excited N^* baryons, we performed a PWA of $\psi(3686) \rightarrow p\bar{p}\pi^0$ [11] and found that the dominant contributions are from 7 N^* intermediate resonances. Among these N^* resonances, two new resonances are significant, one $1/2^+$ resonance with a mass of $2300^{+40+109}_{-30-0} \text{ MeV}/c^2$ and width of $340^{+30+110}_{-30-58} \text{ MeV}$, and one $5/2^-$ resonance with a mass of $2570^{+19+34}_{-10-10} \text{ MeV}/c^2$ and width of $250^{+14+69}_{-24-21} \text{ MeV}$. For the remaining 5 N^* intermediate resonances, the mass and width values from the PWA are consistent with those from established resonances.

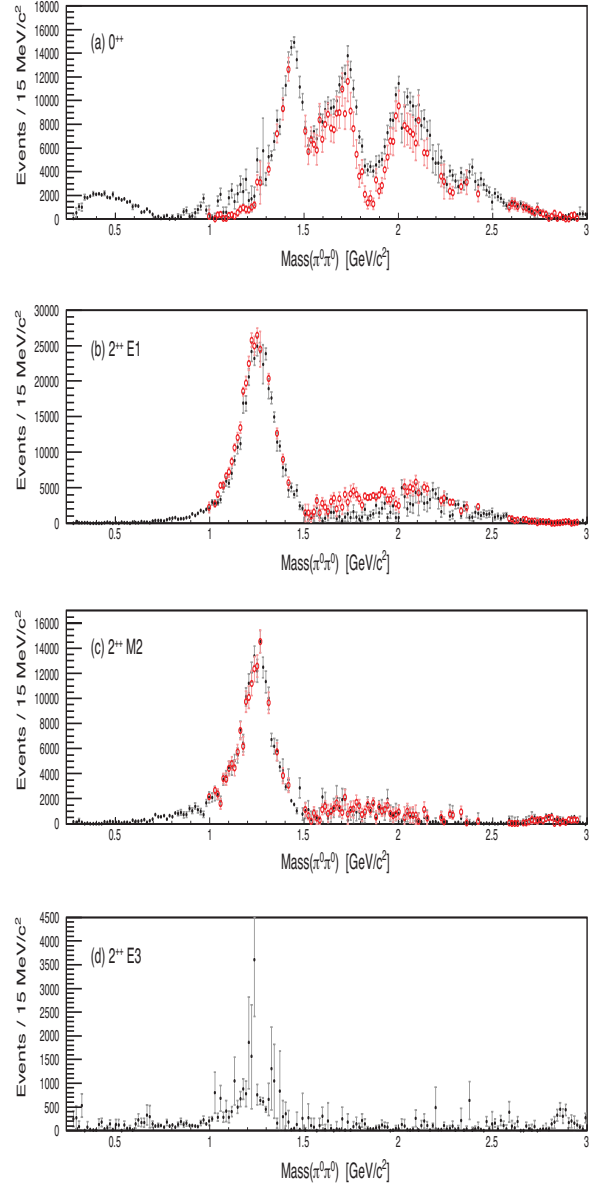


Fig. 2. The intensities for the (a) 0^{++} , (b) 2^{++} E1, (c) 2^{++} M2 and (d) 2^{++} E3 amplitudes as a function of $M_{\pi^0 \pi^0}$ for the nominal results. The solid black markers show the intensity calculated from one set of solutions, while the open red markers represent its ambiguous partner. Note that the intensity of the 2^{++} E3 amplitude is redundant for the two ambiguous solutions.

Using a sample of 1.06×10^8 $\psi(3686)$ events collected at the BESIII detector, the processes of $\psi(3686) \rightarrow K^- \Lambda \bar{\Xi}^+$ and $\psi(3686) \rightarrow \gamma K^- \Lambda \bar{\Xi}^+$ [12] are studied for the first time. In the decay $\psi(3686) \rightarrow K^- \Lambda \bar{\Xi}^+$, the branching fraction $\mathcal{B}(\psi(3686) \rightarrow K^- \Lambda \bar{\Xi}^+)$ is measured, and two structures, around 1690 and 1820 MeV/c^2 , as indicated in Fig. 4, are observed in the $K^- \Lambda$ invariant mass spectrum with significances of 4.9σ and 6.2σ , respectively. The fitted resonance parameters are consistent

with those of $\Xi^-(1690)$ and $\Xi^-(1820)$ in the PDG [13] within one standard deviation. The measured masses, widths are determined to be $M_{\Xi^-(1690)}=1687.7\pm3.8\pm1.0$ MeV/ c^2 , $\Gamma_{\Xi^-(1690)}=27.1\pm10.0\pm2.7$ MeV, $M_{\Xi^-(1820)}=1826.7\pm5.5\pm1.6$ MeV/ c^2 and $\Gamma_{\Xi^-(1820)}=54.4\pm15.7\pm4.2$ MeV. This is the first time that $\Xi^-(1690)$ and $\Xi^-(1820)$ hyperons have been observed in charmonium decays. In the study of the decay $\psi(3686) \rightarrow \gamma K^- \Lambda \Xi^+$, the branching fractions $\mathcal{B}(\psi(3686) \rightarrow K^- \Sigma^0 \Xi^+)$ and $\mathcal{B}(\chi_{cJ} \rightarrow K^- \Lambda \Xi^+)$ are measured. The measurements provide new information on charmonium decays to hyperons and on the resonance parameters of the hyperons, and may help in the understanding of the charmonium decay mechanism.

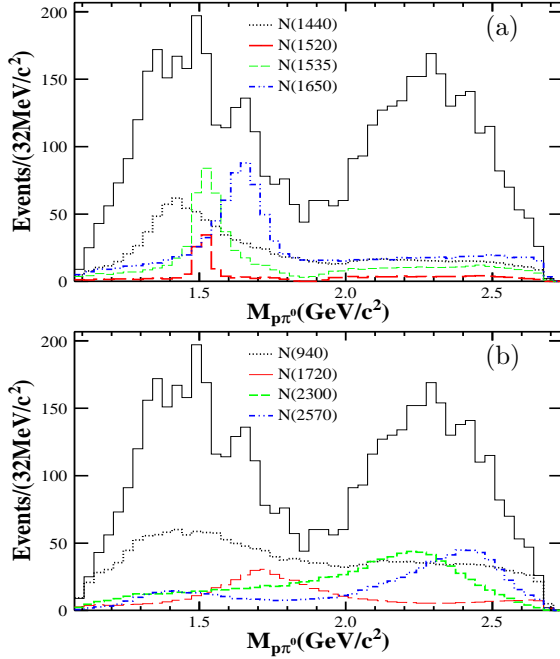


Fig. 3. The contribution of each intermediate resonance in the $p\pi^0$.

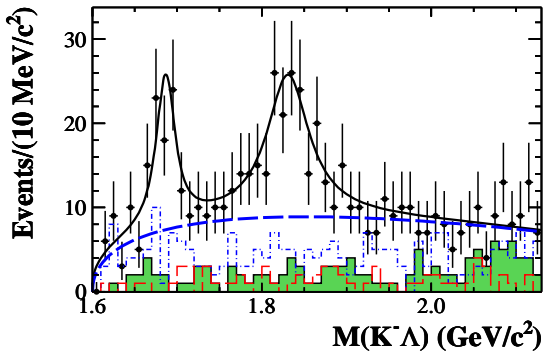


Fig. 4. The contribution of each intermediate resonance in the $p\pi^0$ mass spectra.

4 Light meson decays

Based on a sample of 1.3 billion J/ψ events taken with the BESIII detector, we report the first observation of $\eta' \rightarrow \pi^+\pi^-\pi^+\pi^-$ decays via J/ψ radiative decays [14]. Fig. 5(a) and Fig. 5(b) show the $M_{\pi^+\pi^-\pi^+\pi^-}$ and $M_{\pi^+\pi^-\pi^0\pi^0}$, respectively, where the η' peaks are clearly observed and the dominant background events are from the other η' decays, but none of them contribute to the η' peak. The branching fractions are determined to be $B(\eta' \rightarrow \pi^+\pi^-\pi^+\pi^-)=(8.63\pm0.69\pm0.64)\times10^{-5}$ and $B(\eta' \rightarrow \pi^+\pi^-\pi^0\pi^0)=(1.82\pm0.35\pm0.18)\times10^{-4}$, which are consistent with the theoretical predictions based on the combination of chiral perturbation theory (ChPT) and vector-meson dominance [15], but could rule out the broken- $SU_6 \times O_3$ quark model.

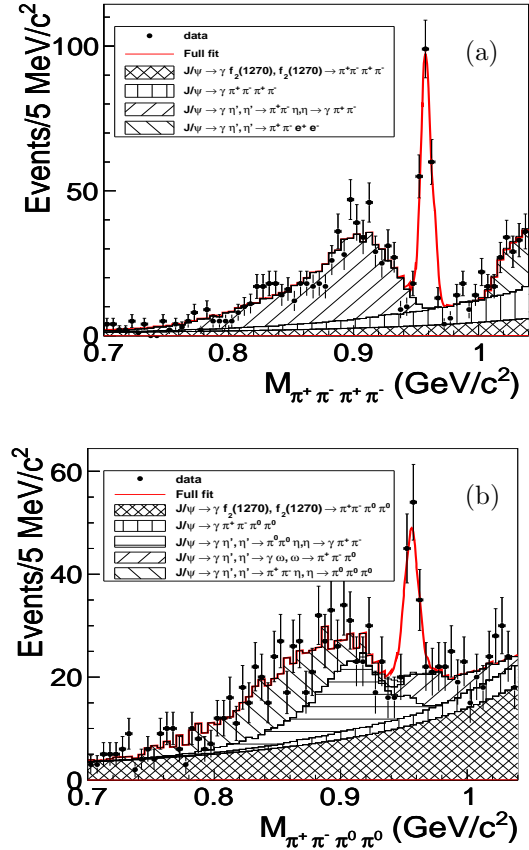


Fig. 5. The invariant mass distributions of (a) $\pi^+\pi^-\pi^+\pi^-$ and (b) $\pi^+\pi^-\pi^0\pi^0$ and the fit results

Recently considerable theoretical efforts to explain the discrepancy that the predicted decay width of $\eta \rightarrow \pi^+\pi^-\pi^0$ at the tree level of chiral perturbation theory (ChPT) is much lower than the experimental value of 300 ± 11 eV [13]. To distinguish between the different theoretical approaches, precise measurements of the matrix elements for $\eta \rightarrow \pi^+\pi^-\pi^0$ and the decay width are

important. At BESIII, a clean sample of 79,625 $\eta \rightarrow \pi^+\pi^-\pi^0$ [16] candidate events are selected and the background contamination is estimated to be about 0.1%. The distribution of X and Y , two the Dalitz plot variables defined as $X = \frac{\sqrt{3}}{Q}(T_{\pi^+} - T_{\pi^-})$ and $Y = \frac{m_\eta + 2m_\pi}{m_\pi} \frac{T_\eta}{Q} - 1$, are shown in Fig. 6 (b) and (c). The Dalitz plot matrix elements for $\eta \rightarrow \pi^+\pi^-\pi^0$ are determined to be $a = -1.128 \pm 0.015 \pm 0.008$, $b = 0.153 \pm 0.017 \pm 0.004$, $d = 0.085 \pm 0.016 \pm 0.009$, $f = 0.173 \pm 0.028 \pm 0.021$, where the first errors are statistical and the second ones systematic. The results are in reasonable agreement with previous measurements.

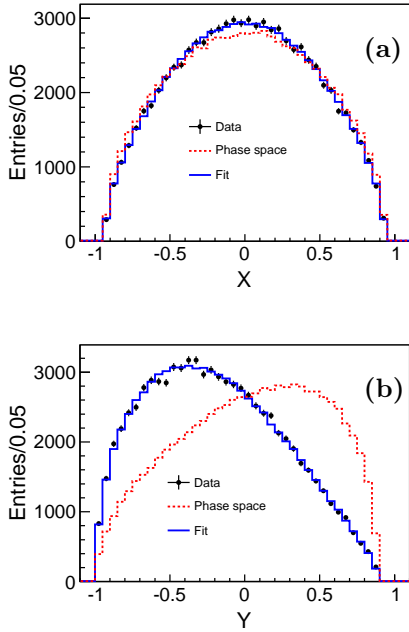


Fig. 6. Projections of the Dalitz plot (a) X and (b) Y for $\eta \rightarrow \pi^+\pi^-\pi^0$.

For the decays of $\eta \rightarrow \pi^0\pi^0\pi^0$, the distribution of the variable Z is displayed in Fig. 7(b). Due to the kinematic boundaries, the interval of $0 < Z < 0.7$, corresponding to the region of phase space in which the Z distribution is flat, is used to extract the slope parameter α from the data. Analogous to the measurement for $\eta \rightarrow \pi^+\pi^-\pi^0$, an unbinned maximum likelihood fit, as displayed in the inset of Fig. 7(a), yields the Dalitz plot slope parameter $\alpha = -0.055 \pm 0.014 \pm 0.004$, which is compatible with the recent results from other experiments and in agreement with the prediction from ChPT at NNLO within two standard deviations of the theoretical uncertainties.

In the same analysis [16], we also presented the Dalitz plot analysis of $\eta' \rightarrow \pi^0\pi^0\pi^0$. The Dalitz plot slope parameter for $\eta' \rightarrow \pi^0\pi^0\pi^0$ is measured to be $\alpha = -0.640 \pm 0.046 \pm 0.047$, which is consistent with but more precise than previous measurements (Fig. 7(b)).

The value deviates significantly from zero. This implies that final state interactions play an important role in the decay. Up to now, there are just a few predictions about the slope parameter of $\eta' \rightarrow \pi^0\pi^0\pi^0$. In Ref. [17], the slope parameter is predicted to be less than 0.03, which is excluded by our measurement. More recently, using a chiral unitary approach, an expansion of the decay amplitude up to the fifth and sixth order of X and Y has been used to parameterize the Dalitz plot of $\eta' \rightarrow \pi^0\pi^0\pi^0$ [18]. The coefficient, which corresponds to α in this paper, is found to be in the range between -2.7 and 0.1 , consistent with our measurement.

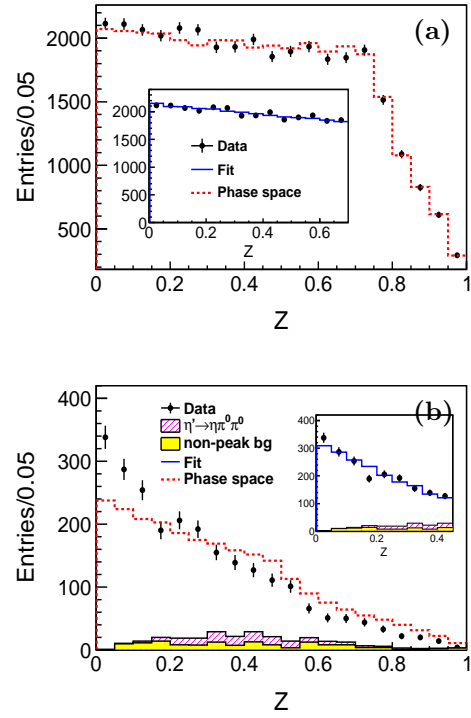


Fig. 7. Distribution of the kinematic variable Z for (a) $\eta \rightarrow \pi^0\pi^0\pi^0$ and (b) $\eta' \rightarrow \pi^0\pi^0\pi^0$.

Theoretically the non-resonant part of coupling in $\eta' \rightarrow \gamma\pi^+\pi^-$ is accounted for by the higher term of Wess-Zumino-Witten (WZW) ChPT Lagrangian[4] (also known as the box anomaly). However the decay dynamics of $h_0 \rightarrow \pi^+\pi^-$ has been explored with very limited statistics only and new measurements are needed to clarify the scenario. In this work, a sample of 9 106 $\eta' \rightarrow \gamma\pi^+\pi^-$ events is selected to investigate its decay dynamics and the $\pi^+\pi^-$ mass spectrum is shown in Fig. 6 with a background level of 1. The shape of the $M_{\pi^+\pi^-}$ spectrum is analyzed in parameterizations with the model-dependent and model-independent approaches respectively. For the model-dependent approach, the results show that only $\rho(770)$ resonance is insufficient to describe the data even considering $\rho(770)$,

ω resonances and the interference between them. The fit performance get much better after including the box anomaly [Fig. 8(a)] with a statistical significance of larger than 37s. We also try to replace the box anomaly with $\rho(1450)$ [Fig. 8 (b)] by fixing its mass the width to be the world average values, the fit seems also can provide a reasonable description of data. Therefore, we conclude that in addition to $\rho(770)$ and ω , the box anomaly is necessary, but the contribution from $\rho(1450)$ could not be ruled out.

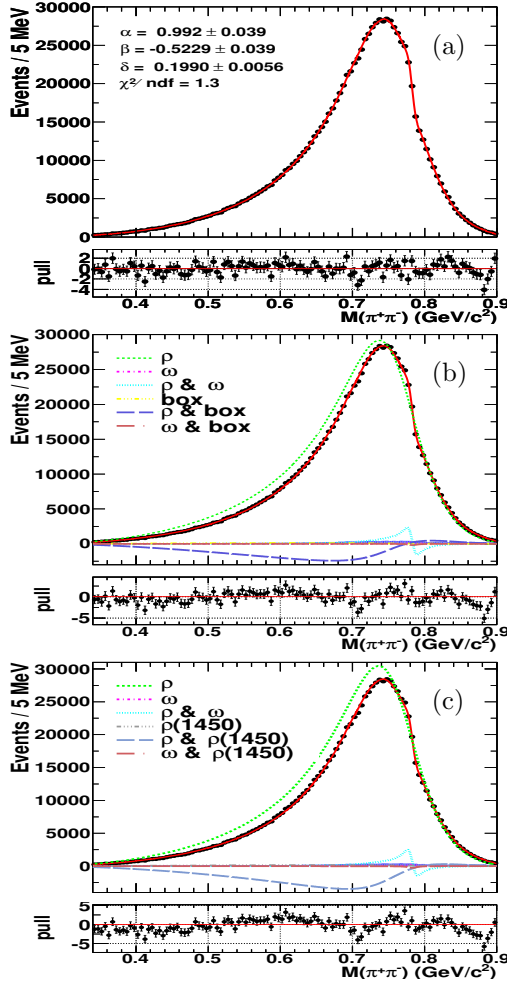


Fig. 8. The fit results for different cases: (a) $\rho(770) - \omega$, (b) $\rho(770) - \omega - \text{box}$ and (c) $\rho(770) - \omega - \rho(1450)$.

5 summary

Based on the data samples taken at the peak of J/ψ , $\psi(3686)$, the recent progresses on the hadron spectroscopy are presented in this talk.

For the light hadron spectroscopy, besides the confirmation of $X(1835)$ in J/ψ radiative decays, the $X(1840)$, is observed in $J/\psi \rightarrow \gamma K_S^0 K_S^0 \eta$. Its spin-parity is determined to be $J^{PC} = 0^{-+}$, which implies that $X(1835)$ is a pseudoscalar resonance. The mass and width are consistent with the previous measurements. In addition, the PWA of $J/\psi \rightarrow \gamma \pi^0 \pi^0$ is performed. For the baryon spectroscopy, two new excited N^* states, $N(2300)$ and $N(2570)$, were observed based on the the PWA of $\psi(3686) \rightarrow p \bar{p} \pi^0$. In addition, the significant progresses on η/η' decays were achieved, including observation of $\eta/\eta' \rightarrow \pi^+ \pi^- \pi^+(0) \pi^-(0)$, Dalitz plot of $\eta \rightarrow \pi^+ \pi^- \pi^0$, $\eta/\eta' \rightarrow 3\pi^0$, and $\eta' \rightarrow \gamma \pi^+ \pi^-$.

The above interesting results not only underline the importance of the study of hadron spectroscopy, but also demonstrate the effectiveness of a programmatic approach to study hadron spectroscopy at BESIII. With the high statistics data accumulated at the BESIII detector, more interesting results are expected to be coming soon.

References

1. M. Ablikim *et al.*, Phys. Rev. Lett. **95**, 262001 (2005).
2. M. Ablikim *et al.*, Phys. Rev. Lett. **106**, 072002 (2011).
3. M. Ablikim *et al.*, Phys. Rev. Lett. **115**, 091803 (2015).
4. M. Ablikim *et al.*, Phys.Rev.Lett. **108**,112003 (2012).
5. M. Ablikim *et al.*, Phys. Rev. Lett. **107**, 182001 (2011).
6. M. Ablikim *et al.*, Phys. Rev. **D 88**, 091502 (2013).
7. M. Ablikim *et al.*, Phys.Rev. **D 87**, 032008 (2013).
8. M. Ablikim *et al.*, Phys. Rev. Lett. **96**, 162002 (2006).
9. M. Ablikim *et al.*, Phys.Rev. **D 92**, 052003 (2015).
10. L. C. Gui *et al.*, Phys.Rev.Lett. **110**, 021601 (2013).
11. M. Ablikim *et al.*, Phys.Rev. Lett. **110**, 021601 (2013).
12. M. Ablikim *et al.*, Phys.Rev. **D 91**, 092006(2015).
13. K. A. Olive *et al.*, Chin. Phys. **C 38**, 1 (2014).
14. M. Ablikim *et al.*, Phys. Rev. Lett. **112**, 251801 (2014).
15. F. K. Guo, B. Kubis and A. Wirzba, Phys. Rev. **D 85**, 014014, (2012).
16. M. Ablikim *et al.*, Phys. Rev. **D 92**, 012014 (2015).
17. C. Roiesnel, T. N. Truong, Paris Ec. Polytech. A **515**, 0982(1982).
18. B. Borasoy, R. Nissler, Eur. Phys. J. A **26**, 383 (2005).